Journal of Computer-Aided Molecular Design (2018) 32:487–496
https://doi.org/10.1007/s10822-018-0103-4

Impact of graphene-based nanomaterials (GBNMs) on the structural and functional conformations of hepcidin peptide

Krishna P. Singh[1,2] · Lokesh Baweja[3] · Olaf Wolkenhauer[4,5] · Qamar Rahman[2] · Shailendra K. Gupta[1,4]

Received: 9 March 2017 / Accepted: 30 January 2018 / Published online: 3 February 2018

Abstract

Graphene-based nanomaterials (GBNMs) are widely used in various industrial and biomedical applications. GBNMs of different compositions, size and shapes are being introduced without thorough toxicity evaluation due to the unavailability of regulatory guidelines. Computational toxicity prediction methods are used by regulatory bodies to quickly assess health hazards caused by newer materials. Due to increasing demand of GBNMs in various size and functional groups in industrial and consumer based applications, rapid and reliable computational toxicity assessment methods are urgently needed. In the present work, we investigate the impact of graphene and graphene oxide nanomaterials on the structural conformations of small hepcidin peptide and compare the materials for their structural and conformational changes. Our molecular dynamics simulation studies revealed conformational changes in hepcidin due to its interaction with GBMNs, which results in a loss of its functional properties. Our results indicate that hepcidin peptide undergo severe structural deformations when superimposed on the graphene sheet in comparison to graphene oxide sheet. These observations suggest that graphene is more toxic than a graphene oxide nanosheet of similar area. Overall, this study indicates that computational methods based on structural deformation, using molecular dynamics (MD) simulations, can be used for the early evaluation of toxicity potential of novel nanomaterials.

Keywords Graphene · Graphene oxide · Hepcidin · Molecular dynamics simulations · Nanotoxicology

Introduction

Graphene-based nanomaterials (GBNMs) such as graphene and graphene oxide (GO) are quite intriguing from both the perspectives of fundamental sciences and advanced material-based technologies. Their chemical nature, thermal tolerance, electrical conductivity, and mechanical properties are of great interest. Owing to these properties, GBNMs have a wide-range of industrial, environmental as well as various biotechnology applications such as adsorbents, catalyst supports, thermal transport media, structural and electronic components, batteries/capacitors, and even applications in biomedicine [1–5]. GO differs from graphene due to the presence of epoxide, hydroyl groups on the surface and carboxyl group at the edges [6], makes it surface partially hydrophilic in nature whereas the surface of graphene is highly hydrophobic. Due to the high affinity of GBNMs for macromolecules such as nucleic acids and proteins, the effect of GBNMs on structural integrity of macromolecules is one of the major concerns [7]. Large numbers of studies investigated the role of nanomaterials in

Olaf Wolkenhauer, Qamar Rahman, Shailendra K. Gupta have contributed equally to this work.

Electronic supplementary material The online version of this article (https://doi.org/10.1007/s10822-018-0103-4) contains supplementary material, which is available to authorized users.

✉ Shailendra K. Gupta
Shailendra.gupta@uni-rostock.de

1 CSIR-Indian Institute of Toxicology Research, 226001 Lucknow, India

2 Amity Institute of Biotechnology, Amity University Uttar Pradesh, Lucknow 226028, Lucknow, India

3 Indian Institute of Technology Gandhinagar, 382355 Gandhinagar, India

4 Department of Systems Biology & Bioinformatics, University of Rostock, 18051 Rostock, Germany

5 Stellenbosch Institute for Advanced Study (STIAS), Wallenberg Research Centre at Stellenbosch University, 7600 Stellenbosch, South Africa

perturbing the native conformation of proteins that lead to the adverse biological consequences such as inhibition of protein function, protein fibrillation and aggregation [8–10]. Several groups are working on computational methods to understand the mechanistic insights of toxicity potential of various nanomaterials [11–15]. Due to increasing demand of GBNMs in various size and functional groups in industrial and consumer based applications, rapid and reliable toxicity assessment methods are urgently needed.

Hepcidin, an eight cysteine-rich cationic peptide detectable in bio fluids including serum and urine, has a simple hairpin like β-sheet structure formed by four disulfide bonds in a ladder-like configuration [8–10, 13]. The proper β-sheet structural orientation of hepcidin is critical for many biological functions such as antibacterial, antifungal activity and iron load metabolism [11]. In the present study, we have investigated the effect of surface chemistries of graphene and GO nanosheets on the bioactive conformation of hepcidin peptide. Small peptide such as hepcidin may serve as a good and rapid model to understand the effect of novel nanomaterials on the functional conformations of biomolecules at atomic scale using molecular dynamics simulations studies. The insights provided by this study have applications for the synthesis of 'safe by design' novel nanomaterials.

Materials and methods

3D confirmation of hepcidin peptide

The coordinates of hepcidin peptide were obtained from the Protein Data Bank (PDB ID: 2KEF) [14]. The small cysteine-rich Peptide form a β-sheet structure with an unusual vicinal disulfide bridge formed at the turn of the hairpin, which is of functional significance for its antibacterial and antifungal activity. In total, three forms of hepcidin are detectable in urine; these are 25, 22 and 20 amino acid residues long. Among them hecpdin-25 is a bioactive form that binds with ferroportin and helps in the internalization and functioning of the protein [12, 15, 16].

Computational models of GBNMs

We established computational models of graphene and GO using the GaussView software V5.0 with a surface area of 25 nm^2 each. The size was selected in a way that it covers the whole hepcidin peptide during a molecular dynamics (MD) simulation run. In case of GO, the surface was randomly decorated with epoxy and hydroxyl groups and the carboxyl groups at the edges were deprotonated to mimic the behavior of GO at physiological pH 7.4 [17]. The ratio of carbon and oxygen (C:O) in GO was set to ~4:1 similar to the experimental settings [6]. In total, there were 1005 carbon and 240 oxygen atoms covalently linked with carbon rings in GO nanosheet of the size 25 nm^2.

3D positioning of hepcidin peptide over graphene and GO

The hepcidin peptide was placed above the surface of graphene and GO at a distance of 5 Å to ignore the possibility of the formation of any intermolecular interactions prior to our MD simulations. These orientations were set using Biovia Materials Studio 7.0 software. In total, we designed three specific sets for hepcidin in complex with GBNMs, these are: (1) Graphene + Hepcidin; (2) Graphene oxide + Hepcidin; and (3) Hepcidin alone, referred as Grap_Hep, GO_Hep and Hep respectively in this manuscript. The initial confirmations of these systems are shown in Fig. 1.

Molecular dynamics simulations

All the three systems (Hep, Grap_Hep and GO_Hep) were studied in detail using molecular dynamics (MD) simulations with the GROMACS software package version (4.5.3) by applying a GROMOS96 53a6 force field. This force-field has been widely used for macromolecule simulation and adjusted partial charges to reproduce hydration free enthalpies in water, recommended for simulations of biomolecules in explicit water [18]. All the systems were solvated with

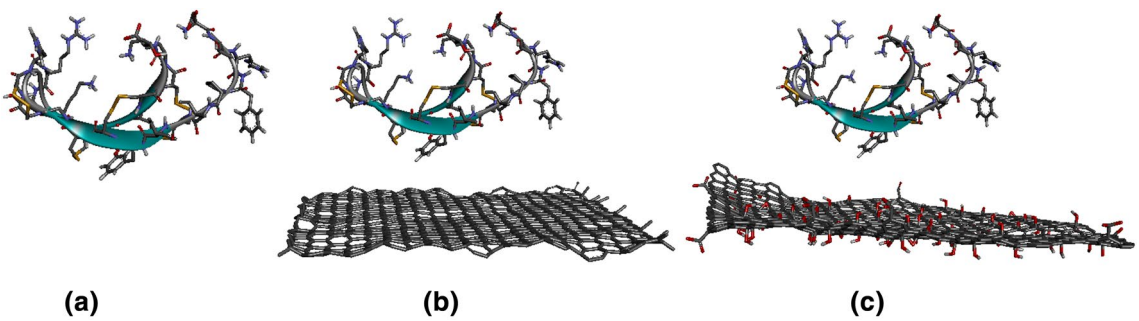

Fig. 1 The initial 3D confirmation of complexes: **a** Hep, **b** Grap_Hep, **c** GO_Hep

single point charge (SPC) water [19]. More specifically, Hep, Grap_Hep and GO_Hep system were solvated in a cubic box ($12 \times 12 \times 12$) nm with periodic boundary conditions containing 57,592, 57,183 and 57,060 number of water molecules respectively. All the three simulation systems were further neutralized using proper counter ions by replacing the water molecules to ensure overall charge neutrality of the system. The systems were equilibrated by 5000 steps of energy minimization using steepest descent algorithm, followed by a 100 picosecond (ps) MD equilibrium simulation in the NVT ensemble, with harmonic restraints (20 kcal mol^{-1} $Å^{-2}$) applied to the backbone atoms of the biomolecules. The entire simulations were performed in the isothermal – isobaric ensemble, and both nanomaterials and peptide were kept unconstrained throughout the simulation run. Temperature and pressure were controlled at 1 atm, and 310 K at same point of time using a Parrinello-Rahman barostat and V-rescale thermostat respectively as described in [19–21]. For the analysis of molecular interactions, a non-bonded cutoff was set to 10 Å and all the electrostatic interactions were calculated using particle mesh Ewald sums [22]. Bonds between hydrogen and heavy atoms were constrained at their equilibrium length using the LINCS algorithm [23]. The production run of 20 ns was performed on all the systems to study conformational changes thoroughly during the simulation run time. All trajectories were saved after each 1 ps interval.

Principal component analysis

Principal component analysis (PCA) was used to obtain the dominant and collective modes of overall motion in the hepcidin peptide, with the help of MD trajectories. Here, the principal components are based on the construction of a mass-weighted covariance matrix of the atom displacement principal. The eigenvector and eigenvalues were extracted with the covariance matrix when diagonalized. This gives information about reflect concerted motion of the molecules [24–26]. We calculated the principal components on the converged simulation and focused on the movement of the 25 Cα atoms of the hepcidin peptide that resulted in 75 dimensional displacement vectors. The PCA method decomposes the overall protein motion into a set of modes (eigenvectors) that are ordered from largest to smallest contributions to the protein fluctuations.

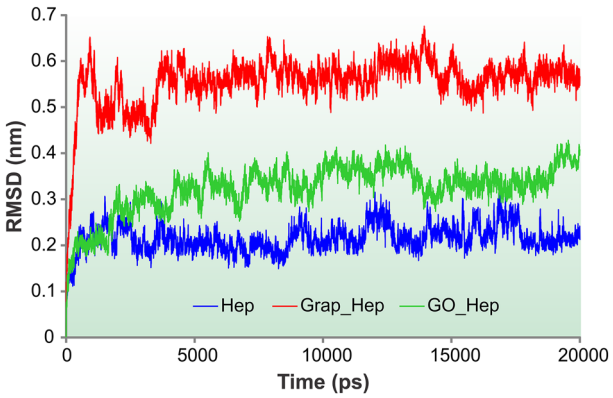

Fig. 2 The root mean square deviation (RMSD) of Cα atoms from hepcidin peptide in three different systems, (1) hepcidin alone (blue color); (2) hepcidin superimposed on graphene (red); and (3) hepcidin superimposed on graphene oxide nanosheet (green). Maximum deviations were observed in case of hepcidin on graphene sheet

Results and discussion

Root-mean-square deviation (RMSD) analyses indicate maximum deviation in hepcidin on graphene sheet

RMSD graph indicates the stability of the system during molecular dynamics simulation run. At each sampling frame, we calculated the RMSD values of Cα atoms of the hepcidin peptide in all the three systems analyzed i.e. Grap_Hep, GO_Hep and Hep. The deviation in Cα atoms was calculated with respect to its initial conformation with the function of time using the Eq. (1):

$$RMSD(t) = \sqrt{\frac{1}{2}\sum_{i=1}^{N}(r_{i(t)} - r_{i(0)})^2} \quad (1)$$

where $r_{i(t)}$ represents the positions of atom i at time t, the same is compared with atom r_i at time 0. N is the total number of backbone atoms.

Based on RMSD graph, it is clear that hepcidin underwent drastic conformational changes during its interaction with graphene as compared to other two systems. Overall, the conformation of the hepcidin peptide without superimposition on nanosheets was conserved throughout the simulation run, which suggests that hepcidin peptide is suitable for addressing the problem of nanomaterial structural and conformational changes prediction undertaken in the present study. Interestingly, significant structural deviations in the hepcidin peptide were observed in the presence of both graphene and graphene oxide nanosheets. In particular, we observed that the RMSD values of Cα atoms in Grap_Hep system increases from 0.1 to 0.6 nm, but in case of GO_Hep it was from 0.1 to 0.4 nm, whereas,

in hepcidin alone, the RMSD was stabilized between 0.1 and 0.2 nm (Fig. 2).

Root mean square fluctuations (RMSF) also suggest that hepcidin amino acid residues have maximum changes when superimposed on graphene

The root mean square fluctuations analysis measures the fluctuation of the bio-molecules during the simulation time. We used g_rmsf tool available in gromacs for the calculation of RMSF values. Based on this analysis, we were interested to identify the fluctuations in the individual amino acid residues of hepcidin peptide in the present or absence of GBNMs as shown in Fig. 3.

The C-terminal residues of hepcidin showed similar fluctuations on graphene and GO nanosheets, whereas, the hepcidin peptide alone was very stable. Our analyses confirm that hepcidin amino acid residues have highest fluctuations in Grap_Hep system in comparison to the GO_Hep and Hep system. The main reason behind the high fluctuation in the hepcidin amino acid residues in the complex systems was the presence of nanosheets on which continues adsorption and desorption of amino acid residues took place during the whole simulation time. Due to several hydrophilic and hydrophobic interactions formed between the hepcidin and GO during the simulation run, the overall fluctuations were low in comparison to the Grap_Hep system which includes only hydrophobic interactions. Overall Fig. 3 clearly indicates that graphene has the highest impact on the structural integrity of hepcidin peptide.

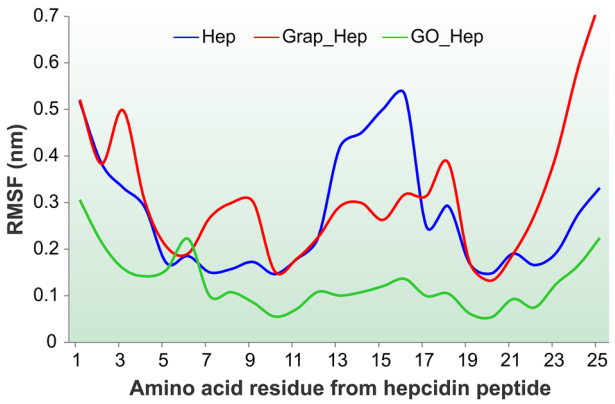

Fig. 3 Root mean square fluctuation (RMSF) plot of the backbone fluctuations obtained for individual amino acid residues of hepcidin peptide in Grap_Hep, GO_Hep and Hep systems over a simulation period of 20 ns

We observed changes in the secondary structure conformations during MD simulation runs

The changes in secondary structure conformations were analyzed by the time-depended secondary structure fluctuations during the 20 ns MD simulation run in all the three systems analyzed. The secondary structure analysis was mainly performed to investigate the effects of the nanomaterial surface chemistry on the peptide conformations. The secondary structure analysis of the hepcidin peptide was performed using DSSP protocol [27] available in the do_dssp module of GROMACS package. In this protocol, hydrogen bonding and other geometrical parameters were used to assign the secondary structure of the peptide. The information retrieved, from the secondary structure analysis, clearly highlight that hepcidin peptide in the Grap_Hep system attains more conformational changes in comparison to GO_Hep and Hep systems. Secondary structure evolution plots illustrate the typical conformational trends exhibited by hepcidin in the presence of graphene, GO and alone as shown in Fig. 4.

After a 20 ns of simulation runs for the Hep system, it was observed that a bulk of amino acid residues retained their original conformation with only minor increase in the in the β-sheet conformations. However, in case of GO_Hep system, the hepcidin had lots of conformational changes in the N- and C-terminus as a result of which the β-sheet conformations get lost. C-terminal residues bend to coil transitions along with some middle residues, while N-terminal residues also exhibit changes in β-sheet conformation. This was in contrast to Grap_Hep, where majority of the amino acid residues lost their structural conformations from β-sheet to coil or helix. The secondary structure analysis shows that majority of amino acid residues present in Hep system tend to form β-sheets throughout the MD simulation run in comparison to Grap_Hep and GO_Hep systems. Also, in case of Grap_Hep and GO_Hep systems, a majority of residues lost their conformations and underwent β-sheet to bend or coil conformations. MD simulation snapshots after 20 ns of GBNMs complex show different conformations as compare to Hep system (Fig. 5).

Intramolecular hydrogen bonds play significant role in determining the structural confirmations of hepcidin peptide superimposed on GBNMs

The Intramolecular hydrogen bond of hepcidin residues were analysed using g_hbond tool available within GROMACS software package. For the hydrogen bonds, we have used cutoff distance ≤ 3.5 Å between donor and acceptor and the cutoff angle between donor and acceptor was set to $> 30°$. The surface chemistry phenomenon was confirmed by the trend of bond formations with hepcidin during its run time.

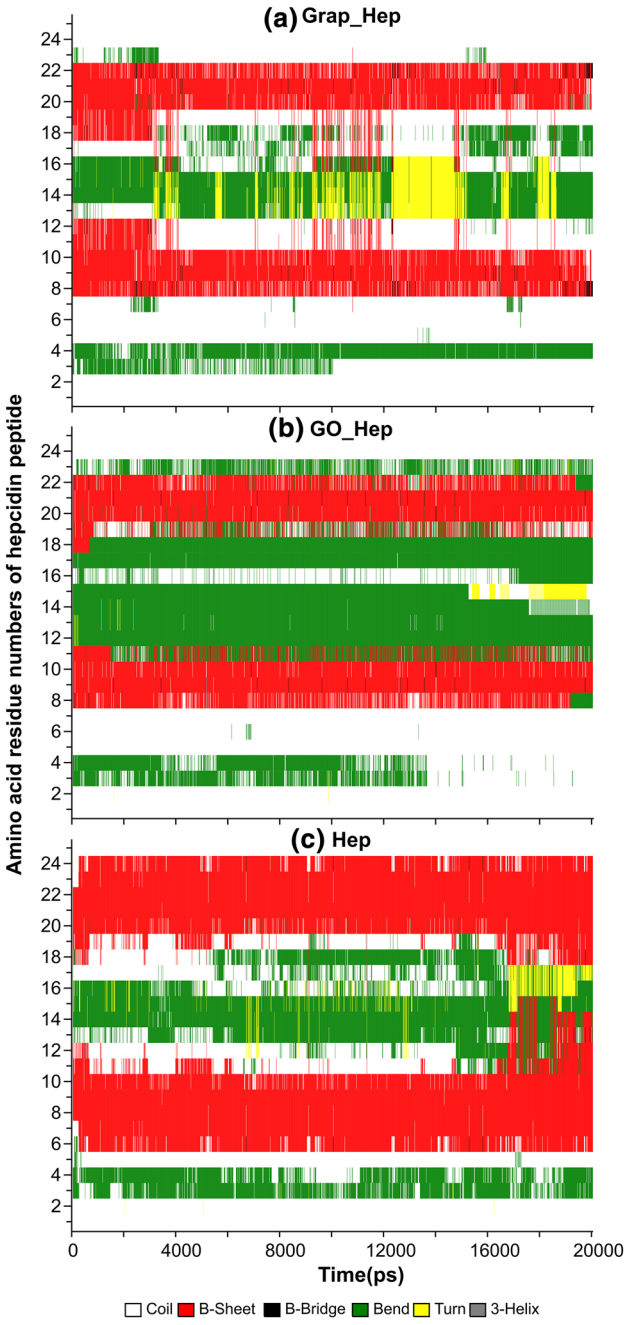

Fig. 4 Secondary structure analyses of the hepcidin peptide during 20 ns MD simulation run in: **a** Grap_Hep, **b** GO_Hep, **c** Hep systems. The graphs indicate that hepcidin underwent maximum structure conformational changes when superimposed on graphene sheet. Overall the β-sheet confirmation, that place crucial role in the hepcidin peptide function, was severely affected when superimposed on GBNMs sheets

In order to find the role of hydrogen bonds in the formation of β sheet, the number of hydrogen bonds between hepcidin residues were analysed at various time points of MD simulations as shown in Fig. 6. In the initial conformations of all the three systems (Hep, GO_Hep, Grap_Hep), the number of hydrogen bonds present in hepcidin were same which changes frequently along with the MD simulation run. As the simulation time increases, the bond formation capacity of hepcidin in both Grap_Hep and GO_Hep systems get reduced and at the end of simulations only small number of hydrogen bonds were retained. This is because of large numbers of intermolecular van der Waal and electrostatic interactions between the GBNMs and hepcidin that resulted in stretched confirmation and loss of intramolecular H-bonds in hepcidin peptide. In contrast, the hepcidin peptide in Hep system showed a trend of increase intramolecular hydrogen bonds, that helped peptide to attain β-sheet conformations as also indicated in the secondary structure analysis in Fig. 4. We observed that the number of intramolecular H-bonds in hepcidin peptide increased in the initial phase of simulation and after 15 ns, reaches to the maximum. The intramolecular H-bonds in hepcidin peptide in all the three systems at initial (0 ns) and final poses (20 ns) are shown in Table 1. It was previously observed that H-bonds between ILE6-LYS24, ILE8-CYS22, CYS10-GLY20 and disulfide bonds between CYS7-CYS23, CYS10-CYS22, CYS11-CYS19, CYS13-CYS14 play important role in the antimicrobial, antifungal and signalling properties in hepcidin in iron metabolism [11]. In our MD simulation run, we found that H-bond between ILE8-CYS22 was conserved throughout the production run in all of the three systems analyzed. We also observed that other intramolecular H-bonds, initially present in the hepcidin peptide, were not conserved after the simulation run when it was superimposed on GBNMs. Interestingly, many new intramolecular H-bonds were formed in hepcidin peptide when it was superimposed on graphene sheet. These bonds were responsible for drastic structural changes in the hepcidin peptide in the Grap_Hep system.

We have also investigated the intermolecular interactions formed between hepcidin peptide and GBNMs sheets (see supplementary Tables 1 and 2). It is obvious that no intermolecular H-bonds formed between hepcidin superimposed on graphene sheet due to the presence of only C-atoms in the graphene. We found that during the adsorption processes of peptide on GBNMs, many conformational changes took place owing to the formation and deletion of hydrogen and disulfide bonds that resulted in the loss of hepcidin β sheet conformation and functional properties.

Solvent-accessible surface area (SASA) of hepcidin increases in GO_Hep and Grap_Hep systems indicating unfolding of peptide when superimposed on GBNMs

In the SASA analysis, we have measured the compactness of the hepcidin peptide by analysing the change in solvent exposed surface area. SASA analysis was performed using g_sas function available in GROMACS on all the three

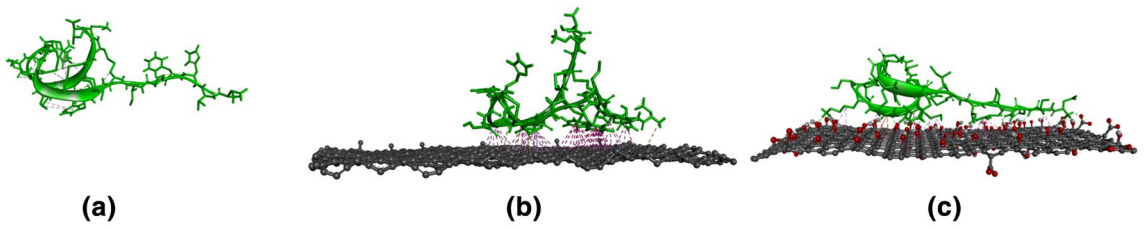

Fig. 5 Conformations of hepcidin obtained at the end of simulation: **a** Hep, **b** Grap_Hep, **c** GO_Hep

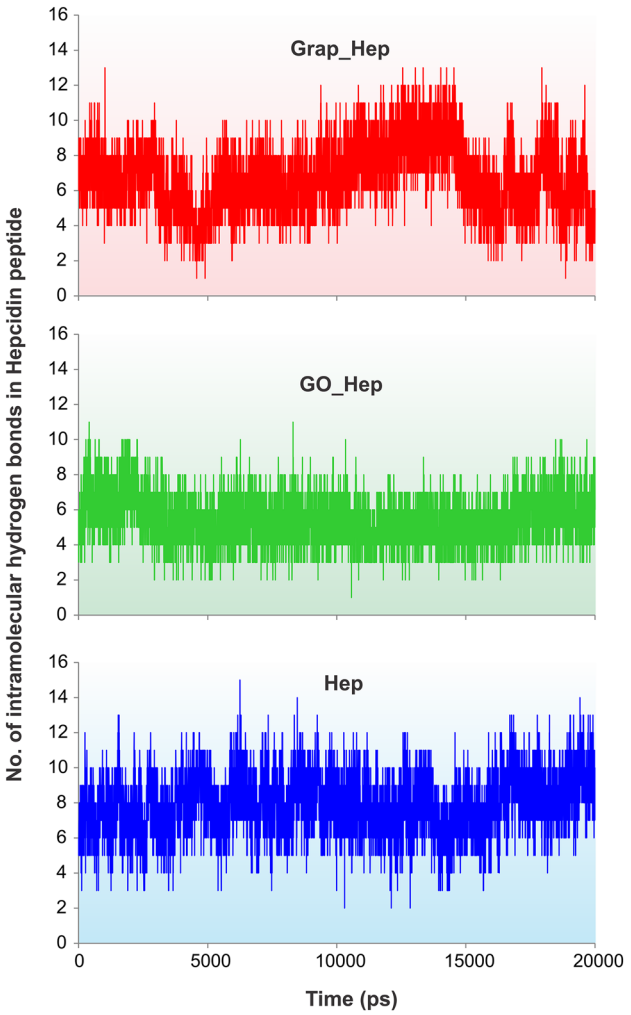

Fig. 6 Change in the number of hydrogen bonds in hepcidin peptide during the simulation run. Blue lines indicate that number of H-bonds increases in the Hep system over a period of time while in other two systems i.e. Grap_Hep (Red) and GO_Hep (Green) a decreasing trend is observed

Table 1 Status of intramolecular H-bonds in the hepcidin peptide during 20 ns MD simulation runs

S. no.	Intramolecular hydrogen bonds in hepcidin peptide	H-bonds at 0 ns	H-bonds at 20 ns		
			Hep	GO_Hep	Grap_Hep
1	ILE8:H—CYS22:O	✓	✓	✓	✓
2	CYS10:H—GLY20:O	✓	✓	✓	×
3	LYS24:H—ILE6:O	✓	✓	×	×
4	CYS7:HA—CYS22:O	✓	×	×	×
5	CYS11:HA—LYS18:O	✓	✓	×	×
6	CYS19:HA—CYS10:O	✓		×	×
7	CYS23:HA—ILE6:O	✓	✓	×	×
8	CYS10:H—ILE8:O	×	✓	×	×
9	GLY12:H—LYS18:O	×	✓	✓	×
10	HIS15:HE2—MET21:O	×	✓	✓	×
11	CYS23:H—MET21:O	×	✓	✓	✓
12	THR25:H—CYS23:O	×	✓	✓	×
13	PRO5:CD—HIS3:O	×	✓	✓	×
14	GLY12:CA—ARG16:O	×	✓	×	×
15	GLY12:CA—SER17:O	×	✓	×	×
16	ILE6:H—PHE4:O	×	×	×	✓
17	PHE9:H—CYS7:O	×	×	×	✓
18	LYS18:H—SER17:OG	×	×	×	✓
19	CYS19:H—SER17:O	×	×	×	✓
20	ARG16:CD—LYS18:O	×	×	×	✓

The ✓ sign indicates that the particular H-bond is present while × indicate that the bond is not present at the observed time point in MD simulations

simulation systems. We calculated both the hydrophobic and hydrophilic SASA and observed that the hydrophobic SASA increased over a period of time when hepcidin peptide was superimposed either on graphene or graphene oxide nanosheets. No change was observed in the SASA of hydrophilic amino acid residues. An increase in the hydrophobic SASA value proves unfolding of the hepcidin peptide during the MD simulations that resulted in the exposure of buried hydrophobic amino acid residues. The SASA of hepcidin in all the three simulation systems is shown in Fig. 7. We observed an increase of hydrophobic SASA value of

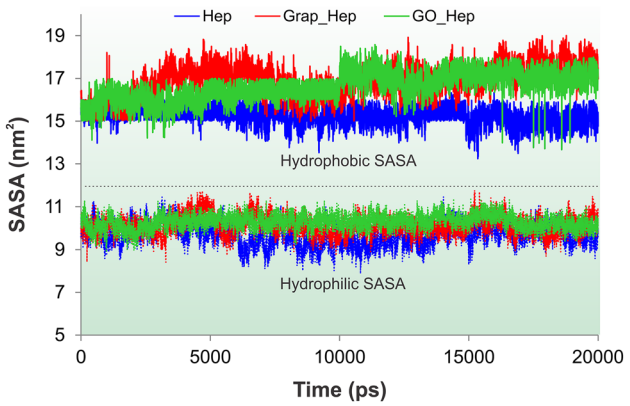

Fig. 7 Change in the solvent accessible surface area (SASA) of hepcidin peptide with respect to time

hepcidin from 15 to 17.5 nm^2 in GO_Hep system and to 18 nm^2 in case of Grap_Hep system after 20 ns simulation run. In an earlier study performed by Guo and colleagues, it was shown that the hydrophobic NMs plays important role in the distortion of β-sheet conformation [28]. The time-dependent increases in SASA of hepcidin peptide absorbed on either of the GBNMs confirm that peptide loses its functional conformations.

Our simulation results also indicate that in both Grap_Hep and GO_Hep systems, the contact surface area of hepcidin with nanomaterials increases (Fig. 8) due to which there is an increase in the hydrophobic π interactions with graphene and GO.

Nonbonded interaction energies of hepcidin with GBNMs in MD simulations

The adsorption of hepcidin on GBNMs is mainly due to the non-bonded interactions such as van der Waals, electrostatic and hydrophobic [17]. The non-bonded interaction energies [van der Waals (vdW) and electrostatic] and total interaction energy between hepcidin and GBNMs revealed different adsorption pattern of peptide, represented in Fig. 9.

The adsorption of hepcidin on GO can mainly be contributed to electrostatic interactions as shown by the significant decrease in electrostatic energy (from − 400 to − 700 kJ/mol) at 15 ns of simulation run that suggest high electrostatic affinity of hepcidin with GO (Fig. 9a). In case of the Grap_Hep system, the vdW energy only contributed in the adsorption process due to the presence of only carbon atoms in the graphene nanosheet. In Fig. 9b, we plotted the total interaction energy [vdW + electrostatic] during the adsorption of hepcidin on GBNMs. We observed that the total interaction energy get stabilized at around 5 ns of simulation run indicating that hepcidin forms stable complexes with GBNMs. On the other hand, hepcidin peptide also indicates different adsorption patterns in GBNMs due to their different surface chemistries.

Principal components analysis

The motions of protein can be classified using PCA analysis [24, 29]. This method is mainly use to reduce the dimensionality of a complex data set as a result complex motions

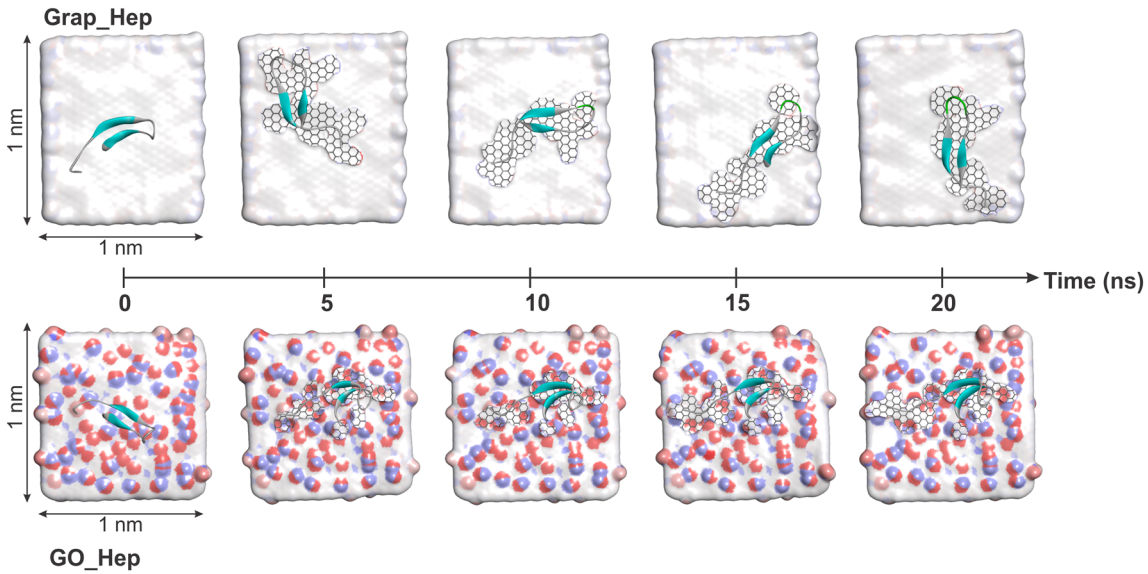

Fig. 8 Hydration patterns of Grap_Hep and GO_Hep complexes at every 5 ns of simulation run. Hepcidin peptide is shown as solid ribbon model. The white color over GBNMs represent water molecules which were displaced during the simulation run. As shown in the figure, displacement of water molecules increases with the increase in hepcidin and GBNMs contact area due to peptide unfolding from 5 to 20 ns

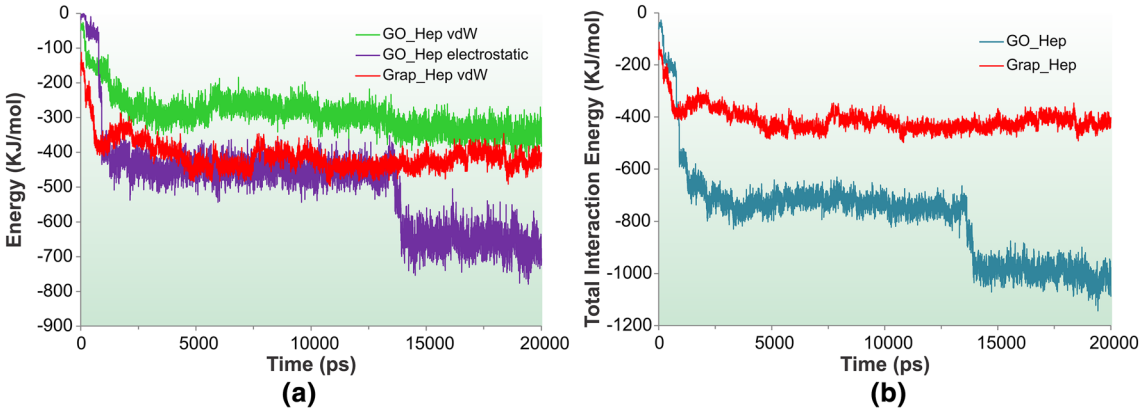

Fig. 9 Nonbonded interaction energies of hepcidin and GBNMs in MD simulations. **a** van der Waals (vdW), electrostatic interaction energies of Grap_Hep (red) and GO_Hep systems (purple and green). It is important to note that in case of Grap_Hep system only vdW energy could be calculated due to the absence of oxygen atoms in the graphene. **b** Total interaction energy in Grap_Hep (vdW) and GO_Hep (vdW + electrostatic) systems

can be decomposed into a few principal motions each of which is represented by eigenvector and eigenvalues. The eigenvalues for a given motion represents the contribution of the corresponding eigenvector to the global motion of the protein as shown in Fig. 10a.

A total of 75 eigenvectors were generated for the entire trajectory indicating that the overall flexibility was calculated by the trace of diagonalized covariance matrix. We calculated the Trace value (the sum of the eigenvalues) of a diagonalizable matrix. The trace values for Grap_Hep, GO_Hep and Hep structure was found to be 2.933, 1.422 and 0.310 nm^2 respectively. Among these values, Grap_Hep showed high values suggesting an overall escalation in the flexibility than the GO_Hep and Hep model, whereas Hep exhibited lowest value confirming the decrease in flexibility in the collective motion of the protein. Approximately, the first 10 eigenvectors (modes) contribute greatly to the collective motions. The first 10 collective modes for each system with cumulative fluctuation percentage are shown in Fig. 10b. The Grap_Hep system shows 95% of motion in first five eigenvectors and in case of GO_Hep, Hep shows 78% and 75% of cumulative motion. The above values indicate that Grap_Hep shows more overall variance in a system as compare to GO_Hep and Hep in the first five eigenvectors of the system.

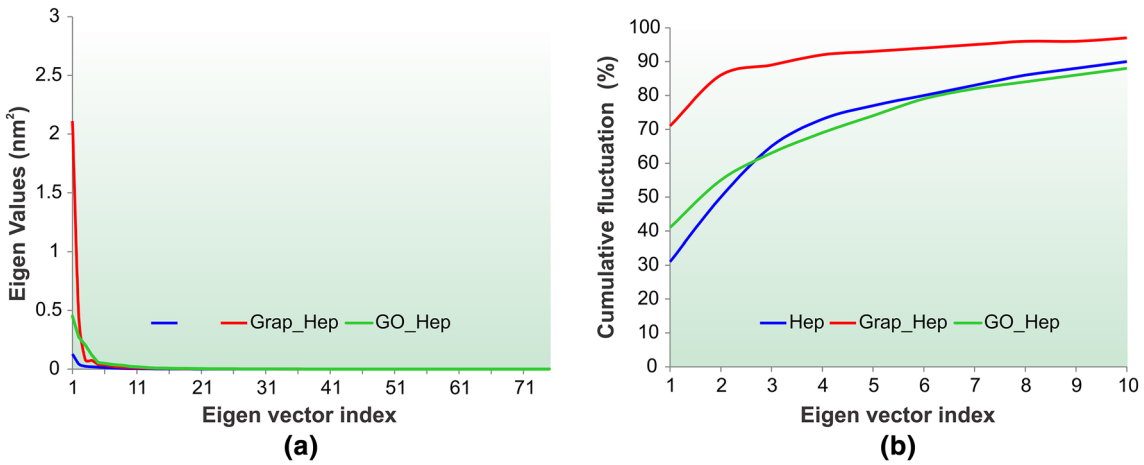

Fig. 10 **a** Plot of eigenvalues corresponding to eigenvector index for the first seventy-five modes of motion of Hepcidin in all systems. **b** Cumulative sum of the contribution to the total fluctuations for first 10 eigenvectors in all the three systems analyzed. Red: Grap_Hep, Green: GO_Hep, Blue: Hep

Conclusions

In this work, we simulated the hepcidin peptide with and without GBNMs to investigate the effect of GBNMs on its β-sheet nature. This specific structural conformation of the peptide plays an important role in the regulation of iron export from enterocytes and macrophages by binding the membrane iron exporter, ferroportin, leading to its internalization and degradation [30]. The detailed simulation analyses for three simulation systems presented in this study proved that hepcidin peptide properly adsorbed on the surface of GBNMs and form stable complexes led to the structural distortion of peptide and loss of its functionality. The overall findings provide insights into the distortion of the β-sheet nature of hepcidin peptide in the presence of GBNMs. The present computational study suggests various parameters to investigate the role of surface chemistry of GBNMs in modulating the structure and function of hepcidin peptide. Among GBNMs, the graphene induces drastic conformational changes in the peptide when compared to a GO nanosheet, which could be the plausible reason for the differential toxic response of GBNMs in biological systems. Moreover, our study suggests that molecular dynamics simulations can be used to assess the structural and conformational changes in small peptides regulating important biological processes due to the exposure of various nanomaterials.

Acknowledgements SKG and KPS acknowledge the Council of Scientific and Industrial Research (CSIR) India Network Projects GENESIS (BSC0121), NANOSHE (BSC0112) and INDEPTH (BSC0111). SKG and OW acknowledge University of Rostock, Rostock, Germany.

Compliance with Ethical Standards

Disclosure of interest The authors report no conflicts of interest.

References

1. Yoo E, Kim J, Hosono E et al (2008) Large reversible Li storage of graphene nanosheet families for use in rechargeable lithium ion batteries. Nano Lett 8:2277–2282. https://doi.org/10.1021/nl800957b
2. Kuila T, Bose S, Khanra P et al (2011) Recent advances in graphene-based biosensors. Biosens Bioelectron 26:4637–4648. https://doi.org/10.1016/j.bios.2011.05.039
3. Shen H, Zhang L, Liu M, Zhang Z (2012) Biomedical applications of graphene. Theranostics 2:283–294. https://doi.org/10.7150/thno.3642
4. Sreeprasad TS, Pradeep T (2012) Graphene for environmental and biological applications. Int J Mod Phys B 26:1242001. https://doi.org/10.1142/S0217979212420015
5. Bao H, Pan Y, Li L (2012) Recent advances in graphene-based nanomaterials for biomedical applications. Nano Life 2:1230001. https://doi.org/10.1142/S179398441100030X
6. Dreyer DR, Park S, Bielawski CW, Ruoff RS (2010) The chemistry of graphene oxide. Chem Soc Rev 39:228–240. https://doi.org/10.1039/b917103g
7. Shemetov AA, Nabiev I, Sukhanova A (2012) Molecular interaction of proteins and peptides with nanoparticles. ACS Nano 6:4585–4602. https://doi.org/10.1021/nn300415x
8. Leong W-I, Lönnerdal B (2004) Hepcidin, the recently identified peptide that appears to regulate iron absorption. J Nutr 134:1–4
9. Rossi E (2005) Hepcidin–the iron regulatory hormone. Clin Biochem Rev 26:47–49
10. Nemeth E, Ganz T (2009) The role of hepcidin in iron metabolism. Acta Haematol 122:78–86. https://doi.org/10.1159/000243791
11. Hunter HN, Fulton DB, Ganz T, Vogel HJ (2002) The solution structure of human hepcidin, a peptide hormone with antimicrobial activity that is involved in iron uptake and hereditary hemochromatosis. J Biol Chem 277:37597–37603. https://doi.org/10.1074/jbc.M205305200
12. Nemeth E, Preza GC, Jung CL et al (2006) The N-terminus of hepcidin is essential for its interaction with ferroportin: structure-function study. Blood 107:328–333. https://doi.org/10.1182/blood-2005-05-2049
13. Kemna EHJM., Tjalsma H, Willems HL, Swinkels DW (2008) Hepcidin: from discovery to differential diagnosis. Haematologica 93:90–97. https://doi.org/10.3324/haematol.11705
14. Jordan JB, Poppe L, Haniu M et al (2009) Hepcidin revisited, disulfide connectivity, dynamics, and structure. J Biol Chem 284:24155–24167. https://doi.org/10.1074/jbc.M109.017764
15. Girelli D, Nemeth E, Swinkels DW (2016) Hepcidin in the diagnosis of iron disorders. Blood 127:2809–2813. https://doi.org/10.1182/blood-2015-12-639112
16. Cenci L, Andreetto E, Vestri A et al (2015) Surface plasmon resonance based on molecularly imprinted nanoparticles for the picomolar detection of the iron regulating hormone Hepcidin-25. J Nanobiotechnol 13:51. https://doi.org/10.1186/s12951-015-0115-3
17. Baweja L, Balamurugan K, Subramanian V, Dhawan A (2013) Hydration patterns of graphene-based nanomaterials (GBNMs) play a major role in the stability of a helical protein: a molecular dynamics simulation study. Langmuir 29:14230–14238. https://doi.org/10.1021/la4033805
18. Oostenbrink C, Villa A, Mark AE, van Gunsteren WF (2004) A biomolecular force field based on the free enthalpy of hydration and solvation: the GROMOS force-field parameter sets 53A5 and 53A6. J Comput Chem 25:1656–1676. https://doi.org/10.1002/jcc.20090
19. Parrinello M (1981) Polymorphic transitions in single crystals: a new molecular dynamics method. J Appl Phys 52:7182. https://doi.org/10.1063/1.328693
20. Nosé S (1984) A unified formulation of the constant temperature molecular dynamics methods. J Chem Phys 81:511. https://doi.org/10.1063/1.447334
21. Bussi G, Donadio D, Parrinello M (2007) Canonical sampling through velocity rescaling. J Chem Phys 126:14101. https://doi.org/10.1063/1.2408420
22. Essmann U, Perera L, Berkowitz ML et al (1995) A smooth particle mesh Ewald method. J Chem Phys 103:8577. https://doi.org/10.1063/1.470117
23. Hess B, Bekker H, Berendsen HJC, Fraaije JGEM (1997) LINCS: a linear constraint solver for molecular simulations. J Comput Chem 18:1463–1472. https://doi.org/10.1002/(SICI)1096-987X(199709)18:12<1463::AID-JCC4>3.0.CO;2-H
24. Amadei A, Linssen ABM, Berendsen HJC (1993) Essential dynamics of proteins. Proteins Struct Funct Genet 17:412–425
25. van Aalten DM, Findlay JB, Amadei A, Berendsen HJ (1995) Essential dynamics of the cellular retinol-binding

protein–evidence for ligand-induced conformational changes. Protein Eng 8:1129–1135
26. Yamaguchi H, van Aalten DM, Pinak M et al (1998) Essential dynamics of DNA containing a cis.syn cyclobutane thymine dimer lesion. Nucleic Acids Res 26:1939–1946
27. Kabsch W, Sander C (1983) Dictionary of protein secondary structure: pattern recognition of hydrogen-bonded and geometrical features. Biopolymers 22:2577–2637. https://doi.org/10.1002/bip.360221211
28. Guo J, Li J, Zhang Y et al (2013) Exploring the influence of carbon nanoparticles on the formation of β-sheet-rich oligomers of IAPP22–28 peptide by molecular dynamics simulation. PLoS ONE 8:e65579. https://doi.org/10.1371/journal.pone.0065579
29. García AE (1992) Large-amplitude nonlinear motions in proteins. Phys Rev Lett 68:2696–2699. https://doi.org/10.1103/PhysRevLett.68.2696
30. Nemeth E, Tuttle MS, Powelson J et al (2004) Hepcidin regulates cellular iron efflux by binding to ferroportin and inducing its internalization. Science 306:2090–2093. https://doi.org/10.1126/science.1104742